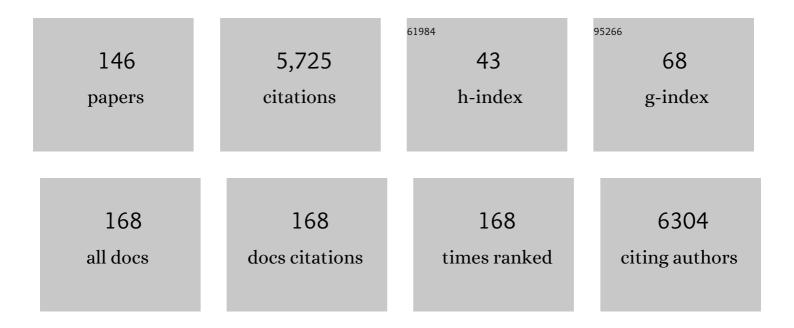
Raymond M Reilly

List of Publications by Year in descending order

Source: https://exaly.com/author-pdf/7678505/publications.pdf Version: 2024-02-01



#	Article	IF	CITATIONS
1	The Effects of Particle Size and Molecular Targeting on the Intratumoral and Subcellular Distribution of Polymeric Nanoparticles. Molecular Pharmaceutics, 2010, 7, 1195-1208.	4.6	302
2	Auger electrons for cancer therapy – a review. EJNMMI Radiopharmacy and Chemistry, 2019, 4, 27.	3.9	196
3	Endothelial apoptosis initiates acute blood-brain barrier disruption after ionizing radiation. Cancer Research, 2003, 63, 5950-6.	0.9	175
4	111In-Labeled Trastuzumab (Herceptin) Modified with Nuclear Localization Sequences (NLS): An Auger Electron-Emitting Radiotherapeutic Agent for HER2/neu-Amplified Breast Cancer. Journal of Nuclear Medicine, 2007, 48, 1357-1368.	5.0	163
5	Problems of Delivery of Monoclonal Antibodies. Clinical Pharmacokinetics, 1995, 28, 126-142.	3.5	151
6	Molecularly targeted gold nanoparticles enhance the radiation response of breast cancer cells and tumor xenografts to X-radiation. Breast Cancer Research and Treatment, 2013, 137, 81-91.	2.5	135
7	Imaging of HER2/neu-positive BT-474 human breast cancer xenografts in athymic mice using 111In-trastuzumab (Herceptin) Fab fragments. Nuclear Medicine and Biology, 2005, 32, 51-58.	0.6	133
8	In Vivo Distribution of Polymeric Nanoparticles at the Whole-Body, Tumor, and Cellular Levels. Pharmaceutical Research, 2010, 27, 2343-2355.	3.5	123
9	Radioimmunotherapy of cancer with high linear energy transfer (LET) radiation delivered by radionuclides emitting α-particles or Auger electrons. Advanced Drug Delivery Reviews, 2017, 109, 102-118.	13.7	117
10	Associations between the uptake of 111In-DTPA-trastuzumab, HER2 density and response to trastuzumab (Herceptin) in athymic mice bearing subcutaneous human tumour xenografts. European Journal of Nuclear Medicine and Molecular Imaging, 2009, 36, 81-93.	6.4	108
11	Oral Delivery of Antibodies. Clinical Pharmacokinetics, 1997, 32, 313-323.	3.5	107
12	Design and Characterization of HER-2-Targeted Gold Nanoparticles for Enhanced X-radiation Treatment of Locally Advanced Breast Cancer. Molecular Pharmaceutics, 2010, 7, 2194-2206.	4.6	107
13	Carbon Nanotubes: Potential Benefits and Risks of Nanotechnology in Nuclear Medicine. Journal of Nuclear Medicine, 2007, 48, 1039-1042.	5.0	103
14	Optimized digital counting colonies of clonogenic assays using ImageJ software and customized macros: Comparison with manual counting. International Journal of Radiation Biology, 2011, 87, 1135-1146.	1.8	97
15	Intratumorally Injected ¹⁷⁷ Lu-Labeled Gold Nanoparticles: Gold Nanoseed Brachytherapy with Application for Neoadjuvant Treatment of Locally Advanced Breast Cancer. Journal of Nuclear Medicine, 2016, 57, 936-942.	5.0	92
16	Role of Antibody-Mediated Tumor Targeting and Route of Administration in Nanoparticle Tumor Accumulation in Vivo. Molecular Pharmaceutics, 2012, 9, 2168-2179.	4.6	90
17	MR-guided focused ultrasound enhances delivery of trastuzumab to Her2-positive brain metastases. Science Translational Medicine, 2021, 13, eabj4011.	12.4	82
18	Noninvasive Monitoring of the Fate of ¹¹¹ In-Labeled Block Copolymer Micelles by High Resolution and High Sensitivity MicroSPECT/CT Imaging. Molecular Pharmaceutics, 2009, 6, 581-592.	4.6	78

#	Article	IF	CITATIONS
19	Micro-SPECT/CT with ¹¹¹ In-DTPA-Pertuzumab Sensitively Detects Trastuzumab-Mediated <i>HER2</i> Downregulation and Tumor Response in Athymic Mice Bearing MDA-MB-361 Human Breast Cancer Xenografts. Journal of Nuclear Medicine, 2009, 50, 1340-1348.	5.0	76
20	Computational analysis of the number, area and density of γ-H2AX foci in breast cancer cells exposed to ¹¹¹ In-DTPA-hEGF or γ-rays using Image-J software. International Journal of Radiation Biology, 2009, 85, 262-271.	1.8	74
21	Trastuzumab-Resistant Breast Cancer Cells Remain Sensitive to the Auger Electron–Emitting Radiotherapeutic Agent 111In-NLS-Trastuzumab and Are Radiosensitized by Methotrexate. Journal of Nuclear Medicine, 2008, 49, 1498-1505.	5.0	73
22	Oncolytic Vaccinia Virus Expressing the Human Somatostatin Receptor SSTR2: Molecular Imaging after Systemic Delivery Using 111In-Pentetreotide. Molecular Therapy, 2004, 10, 553-561.	8.2	72
23	Nuclear localizing sequences promote nuclear translocation and enhance the radiotoxicity of the anti-CD33 monoclonal antibody HuM195 labeled with 1111n in human myeloid leukemia cells. Journal of Nuclear Medicine, 2006, 47, 827-36.	5.0	69
24	In vitro andin vivo evaluation of WK-X-34, a novel inhibitor of P-glycoprotein and BCRP, using radio imaging techniques. International Journal of Cancer, 2006, 119, 414-422.	5.1	67
25	Radiation Nanomedicine for EGFR-Positive Breast Cancer: Panitumumab-Modified Gold Nanoparticles Complexed to the β-Particle-Emitter, ¹⁷⁷ Lu. Molecular Pharmaceutics, 2015, 12, 3963-3972.	4.6	67
26	lmaging of HER2/neu expression in BT-474 human breast cancer xenografts in athymic mice using [99mTc]-HYNIC-trastuzumab (Herceptin) Fab fragments. Nuclear Medicine Communications, 2005, 26, 427-432.	1.1	64
27	111In-labeled trastuzumab-modified gold nanoparticles are cytotoxic in vitro to HER2-positive breast cancer cells and arrest tumor growth in vivo in athymic mice after intratumoral injection. Nuclear Medicine and Biology, 2016, 43, 818-826.	0.6	63
28	Antitumor Effects and Normal-Tissue Toxicity of ¹¹¹ In-Nuclear Localization Sequence-Trastuzumab in Athymic Mice Bearing <i>HER</i> -Positive Human Breast Cancer Xenografts. Journal of Nuclear Medicine, 2010, 51, 1084-1091.	5.0	61
29	Local Radiation Treatment of HER2-Positive Breast Cancer Using Trastuzumab-Modified Gold Nanoparticles Labeled with 177Lu. Pharmaceutical Research, 2017, 34, 579-590.	3.5	61
30	Cellular Dosimetry of ¹¹¹ In Using Monte Carlo N-Particle Computer Code: Comparison with Analytic Methods and Correlation with In Vitro Cytotoxicity. Journal of Nuclear Medicine, 2010, 51, 462-470.	5.0	59
31	Apoptotic Epidermal Growth Factor (EGF)-Conjugated Block Copolymer Micelles as a Nanotechnology Platform for Targeted Combination Therapy. Molecular Pharmaceutics, 2007, 4, 769-781.	4.6	57
32	Relationship Between Induction of Phosphorylated H2AX and Survival in Breast Cancer Cells Exposed to ¹¹¹ In-DTPA-hEGF. Journal of Nuclear Medicine, 2008, 49, 1353-1361.	5.0	57
33	Update:Peptide Motifs for Insertion of Radiolabeled Biomolecules into Cells and Routing to the Nucleus for Cancer Imaging or Radiotherapeutic Applications. Cancer Biotherapy and Radiopharmaceuticals, 2008, 23, 3-24.	1.0	55
34	Block Copolymer Micelles Target Auger Electron Radiotherapy to the Nucleus of HER2-Positive Breast Cancer Cells. Biomacromolecules, 2012, 13, 455-465.	5.4	53
35	Antitumor effects and normal tissue toxicity of 1111n-labeled epidermal growth factor administered to athymic mice bearing epidermal growth factor receptor-positive human breast cancer xenografts. Journal of Nuclear Medicine, 2003, 44, 1469-78.	5.0	53
36	Preclinical pharmacokinetic, biodistribution, toxicology, and dosimetry studies of 111In-DTPA-human epidermal growth factor: an auger electron-emitting radiotherapeutic agent for epidermal growth factor receptor-positive breast cancer. Journal of Nuclear Medicine, 2006, 47, 1023-31.	5.0	51

#	Article	IF	CITATIONS
37	Drug-Resistant AML Cells and Primary AML Specimens Are Killed by ¹¹¹ In-Anti-CD33 Monoclonal Antibodies Modified with Nuclear Localizing Peptide Sequences. Journal of Nuclear Medicine, 2008, 49, 1546-1554.	5.0	50
38	Methotrexate, Paclitaxel, and Doxorubicin Radiosensitize <i>HER2</i> -Amplified Human Breast Cancer Cells to the Auger Electron–Emitting Radiotherapeutic Agent ¹¹¹ In-NLS-Trastuzumab. Journal of Nuclear Medicine, 2010, 51, 477-483.	5.0	49
39	Detection of P-glycoprotein activity in endotoxemic rats by 99mTc-sestamibi imaging. Journal of Nuclear Medicine, 2005, 46, 1537-45.	5.0	49
40	111In-Bn-DTPA-nimotuzumab with/without modification with nuclear translocation sequence (NLS) peptides: an Auger electron-emitting radioimmunotherapeutic agent for EGFR-positive and trastuzumab (Herceptin)-resistant breast cancer. Breast Cancer Research and Treatment, 2012, 135, 189-200.	2.5	47
41	Investigating the influence of block copolymer micelle length on cellular uptake and penetration in a multicellular tumor spheroid model. Nanoscale, 2021, 13, 280-291.	5.6	47
42	Intraperitoneal therapy of malignant ascites associated with carcinoma of ovary and breast using radioiodinated monoclonal antibody 2G3. Gynecologic Oncology, 1992, 47, 102-109.	1.4	46
43	1231-labeled HIV-1 tat peptide radioimmunoconjugates are imported into the nucleus of human breast cancer cells and functionally interact in vitro and in vivo with the cyclin-dependent kinase inhibitor, p21WAF-1/Cip-1. European Journal of Nuclear Medicine and Molecular Imaging, 2007, 34, 368-377.	6.4	46
44	Active Targeting of Block Copolymer Micelles with Trastuzumab Fab Fragments and Nuclear Localization Signal Leads to Increased Tumor Uptake and Nuclear Localization in HER2-Overexpressing Xenografts. Molecular Pharmaceutics, 2013, 10, 4229-4241.	4.6	45
45	Cellular penetration and nuclear importation properties of 111In-labeled and 123I-labeled HIV-1 tat peptide immunoconjugates in BT-474 human breast cancer cells. Nuclear Medicine and Biology, 2007, 34, 37-46.	0.6	42
46	Effect of the EGFR density of breast cancer cells on nuclear importation, in vitro cytotoxicity, and tumor and normal-tissue uptake of [111In]DTPA-hEGF. Nuclear Medicine and Biology, 2007, 34, 887-896.	0.6	41
47	A human transferrin-vascular endothelial growth factor (hnTf-VEGF) fusion protein containing an integrated binding site for (111)In for imaging tumor angiogenesis. Journal of Nuclear Medicine, 2005, 46, 1745-52.	5.0	41
48	Auger Electron Radioimmunotherapeutic Agent Specific for the CD123 ⁺ /CD131 ^{â^'} Phenotype of the Leukemia Stem Cell Population. Journal of Nuclear Medicine, 2011, 52, 1465-1473.	5.0	40
49	Development and preclinical studies of ⁶⁴ Cu-NOTA-pertuzumab F(abâ€2) ₂ for imaging changes in tumor HER2 expression associated with response to trastuzumab by PET/CT. MAbs, 2017, 9, 154-164.	5.2	39
50	Panitumumab Modified with Metal-Chelating Polymers (MCP) Complexed to ¹¹¹ In and ¹⁷⁷ Lu—An EGFR-Targeted Theranostic for Pancreatic Cancer. Molecular Pharmaceutics, 2018, 15, 1150-1159.	4.6	39
51	Dual-Receptor–Targeted Radioimmunotherapy of Human Breast Cancer Xenografts in Athymic Mice Coexpressing HER2 and EGFR Using ¹⁷⁷ Lu- or ¹¹¹ In-Labeled Bispecific Radioimmunoconjugates. Journal of Nuclear Medicine, 2016, 57, 444-452.	5.0	38
52	Site-specific conjugation of HIV-1 tat peptides to IgG: a potential route to construct radioimmunoconjugates for targeting intracellular and nuclear epitopes in cancer. European Journal of Nuclear Medicine and Molecular Imaging, 2006, 33, 301-310.	6.4	37
53	The level of insulin growth factor-1 receptor expression is directly correlated with the tumor uptake of 111In-IGF-1(E3R) in vivo and the clonogenic survival of breast cancer cells exposed in vitro to trastuzumab (Herceptin). Nuclear Medicine and Biology, 2008, 35, 645-653.	0.6	36
54	¹⁸ F-FDG Small-Animal PET/CT Differentiates Trastuzumab-Responsive from Unresponsive Human Breast Cancer Xenografts in Athymic Mice. Journal of Nuclear Medicine, 2009, 50, 1848-1856.	5.0	36

#	Article	IF	CITATIONS
55	Influence of formulation variables on the biodistribution of multifunctional block copolymer micelles. Journal of Controlled Release, 2012, 157, 366-374.	9.9	36
56	Epidermal Growth Factor Receptor Inhibition Modulates the Nuclear Localization and Cytotoxicity of the Auger Electron Emitting Radiopharmaceutical 111In-DTPA Human Epidermal Growth Factor. Journal of Nuclear Medicine, 2007, 48, 1562-1570.	5.0	35
57	MicroPET/CT imaging of patient-derived pancreatic cancer xenografts implanted subcutaneously or orthotopically in NOD-scid mice using 64Cu-NOTA-panitumumab F(ab')2 fragments. Nuclear Medicine and Biology, 2015, 42, 71-77.	0.6	35
58	Synthesis of Polyglutamide-Based Metal-Chelating Polymers and Their Site-Specific Conjugation to Trastuzumab for Auger Electron Radioimmunotherapy. Biomacromolecules, 2014, 15, 2027-2037.	5.4	34
59	A comparison of 111In- or 64Cu-DOTA-trastuzumab Fab fragments for imaging subcutaneous HER2-positive tumor xenografts in athymic mice using microSPECT/CT or microPET/CT. EJNMMI Research, 2011, 1, 15.	2.5	33
60	Investigation of the effects of cell model and subcellular location of gold nanoparticles on nuclear dose enhancement factors using Monte Carlo simulation. Medical Physics, 2013, 40, 114101.	3.0	32
61	Stability and Biodistribution of Thiol-Functionalized and ¹⁷⁷ Lu-Labeled Metal Chelating Polymers Bound to Gold Nanoparticles. Biomacromolecules, 2016, 17, 1292-1302.	5.4	32
62	Comparative antiproliferative effects of 1111n-DTPA-hEGF, chemotherapeutic agents and γ-radiation on EGFR-positive breast cancer cells. Nuclear Medicine and Biology, 2002, 29, 693-699.	0.6	30
63	Multifunctional Block Copolymer Micelles for the Delivery of ¹¹¹ In to EGFR-Positive Breast Cancer Cells for Targeted Auger Electron Radiotherapy. Molecular Pharmaceutics, 2010, 7, 177-186.	4.6	30
64	The human polynucleotide kinase/phosphatase (hPNKP) inhibitor A12B4C3 radiosensitizes human myeloid leukemia cells to Auger electron-emitting anti-CD123 111In-NLS-7G3 radioimmunoconjugates. Nuclear Medicine and Biology, 2014, 41, 377-383.	0.6	30
65	Small-Animal SPECT/CT of HER2 and HER3 Expression in Tumor Xenografts in Athymic Mice Using Trastuzumab Fab–Heregulin Bispecific Radioimmunoconjugates. Journal of Nuclear Medicine, 2012, 53, 1943-1950.	5.0	29
66	Monte Carlo N-Particle (MCNP) Modeling of the Cellular Dosimetry of ⁶⁴ Cu: Comparison with MIRDcell S Values and Implications for Studies of Its Cytotoxic Effects. Journal of Nuclear Medicine, 2017, 58, 339-345.	5.0	29
67	Metal-Chelating Polymers (MCPs) with Zwitterionic Pendant Groups Complexed to Trastuzumab Exhibit Decreased Liver Accumulation Compared to Polyanionic MCP Immunoconjugates. Biomacromolecules, 2015, 16, 3613-3623.	5.4	28
68	Molecular imaging in drug development: Update and challenges for radiolabeled antibodies and nanotechnology. Methods, 2017, 130, 23-35.	3.8	28
69	Phase I trial to evaluate the tumor and normal tissue uptake, radiation dosimetry and safety of (111)In-DTPA-human epidermal growth factor in patients with metastatic EGFR-positive breast cancer. American Journal of Nuclear Medicine and Molecular Imaging, 2014, 4, 181-92.	1.0	27
70	Trastuzumab Labeled to High Specific Activity with ¹¹¹ In by Site-Specific Conjugation to a Metal-Chelating Polymer Exhibits Amplified Auger Electron-Mediated Cytotoxicity on HER2-Positive Breast Cancer Cells. Molecular Pharmaceutics, 2015, 12, 1951-1960.	4.6	26
71	64Cu-Labeled Trastuzumab Fab-PEC24-EGF Radioimmunoconjugates Bispecific for HER2 and EGFR: Pharmacokinetics, Biodistribution, and Tumor Imaging by PET in Comparison to Monospecific Agents. Molecular Pharmaceutics, 2017, 14, 492-501.	4.6	26
72	Effect of Pendant Group Structure on the Hydrolytic Stability of Polyaspartamide Polymers under Physiological Conditions. Biomacromolecules, 2012, 13, 1296-1306.	5.4	25

#	Article	IF	CITATIONS
73	Pretargeted tumour imaging with streptavidin immunoconjugates of monoclonal antibody CC49 and 111In-DTPA-biocytin. Nuclear Medicine and Biology, 1996, 23, 459-466.	0.6	24
74	Trastuzumab Labeled to High Specific Activity with 1111n by Conjugation to G4 PAMAM Dendrimers Derivatized with Multiple DTPA Chelators Exhibits Increased Cytotoxic Potency on HER2-Positive Breast Cancer Cells. Pharmaceutical Research, 2013, 30, 1999-2009.	3.5	24
75	A kit formulated under good manufacturing practices for labeling human epidermal growth factor with 1111n for radiotherapeutic applications. Journal of Nuclear Medicine, 2004, 45, 701-8.	5.0	24
76	Novel tetrahydroisoquinolin-ethyl-phenylamine based multidrug resistance inhibitors with broad-spectrum modulating properties. Cancer Chemotherapy and Pharmacology, 2006, 59, 61-69.	2.3	23
77	Phase I trial of intraoperative detection of tumor margins in patients with HER2-positive carcinoma of the breast following administration of 111In-DTPA-trastuzumab Fab fragments. Nuclear Medicine and Biology, 2013, 40, 630-637.	0.6	22
78	A New Radioligand for the Epidermal Growth Factor Receptor: 111In-Labeled Human Epidermal Growth Factor Derivatized with a Bifunctional Metal-Chelating Peptide. Bioconjugate Chemistry, 1995, 6, 683-690.	3.6	21
79	In vitro and in vivo evaluation of streptavidin immunoconjugates of the second generation TAG-72 monoclonal antibody CC49. Nuclear Medicine and Biology, 1995, 22, 77-86.	0.6	20
80	MicroSPECT/CT imaging of co-expressed HER2 and EGFR on subcutaneous human tumor xenografts in athymic mice using 111In-labeled bispecific radioimmunoconjugates. Breast Cancer Research and Treatment, 2013, 138, 709-718.	2.5	20
81	Amplified delivery of indium-111 to EGFR-positive human breast cancer cells. Nuclear Medicine and Biology, 2001, 28, 895-902.	0.6	19
82	HIV-1 Tat Peptide Immunoconjugates Differentially Sensitize Breast Cancer Cells to Selected Antiproliferative Agents That Induce the Cyclin-Dependent Kinase Inhibitor p21WAF-1/CIP-1. Bioconjugate Chemistry, 2006, 17, 1280-1287.	3.6	19
83	A kit to prepare 111In-DTPA-trastuzumab (Herceptin) Fab fragments injection under GMP conditions for imaging or radioimmunoguided surgery of HER2-positive breast cancer. Nuclear Medicine and Biology, 2011, 38, 129-136.	0.6	19
84	Intracellular Routing in Breast Cancer Cells of Streptavidin-Conjugated Trastuzumab Fab Fragments Linked to Biotinylated Doxorubicin-Functionalized Metal Chelating Polymers. Biomacromolecules, 2014, 15, 715-725.	5.4	19
85	Pre-operative assessment of axillary lymph node status in patients with breast adenocarcinoma using intravenous 99mtechnetium mAb-170H.82 (Tru-Scint®AD™). Breast Cancer Research and Treatment, 1997, 45, 29-37.	2.5	18
86	Properties of [1111n]-labeled HIV-1 tat peptide radioimmunoconjugates in tumor-bearing mice following intravenous or intratumoral injection. Nuclear Medicine and Biology, 2008, 35, 101-110.	0.6	18
87	111In- or 99mTc-labeled recombinant VEGF bioconjugates: in vitro evaluation of their cytotoxicity on porcine aortic endothelial cells overexpressing Flt-1 receptors. Nuclear Medicine and Biology, 2010, 37, 105-115.	0.6	18
88	CD16 ⁺ NK-92 and anti-CD123 monoclonal antibody prolongs survival in primary human acute myeloid leukemia xenografted mice. Haematologica, 2018, 103, 1720-1729.	3.5	18
89	Development of an Epidermal Growth Factor Derivative with EGFR Blocking Activity. PLoS ONE, 2013, 8, e69325.	2.5	18
90	Synthesis and preliminary biological evaluations of [18F]-1-deoxy-1-fluoro-scyllo-inositol. Chemical Communications, 2009, , 5527.	4.1	17

#	Article	IF	CITATIONS
91	Positron-Emission Tomography Imaging of the TSPO with [¹⁸ F]FEPPA in a Preclinical Breast Cancer Model. Cancer Biotherapy and Radiopharmaceuticals, 2013, 28, 254-259.	1.0	17
92	Biopharmaceuticals as Targeting Vehicles forIn situ Radiotherapy of Malignancies. , 0, , 497-535.		17
93	Radioimmunotherapy of solid tumors: the promise of pretargeting strategies using bispecific antibodies and radiolabeled haptens. Journal of Nuclear Medicine, 2006, 47, 196-9.	5.0	17
94	ErbB-2 Blockade and Prenyltransferase Inhibition Alter Epidermal Growth Factor and Epidermal Growth Factor Receptor Trafficking and Enhance ¹¹¹ In-DTPA-hEGF Auger Electron Radiation Therapy. Journal of Nuclear Medicine, 2011, 52, 776-783.	5.0	16
95	The Effect of Metal-Chelating Polymers (MCPs) for 111In Complexed via the Streptavidin-Biotin System to Trastuzumab Fab Fragments on Tumor and Normal Tissue Distribution in Mice. Pharmaceutical Research, 2013, 30, 104-116.	3.5	16
96	MicroSPECT/CT imaging of primary human AML engrafted into the bone marrow and spleen of NOD/SCID mice using 111In-DTPA-NLS-CSL360 radioimmunoconjugates recognizing the CD123+/CD131â^' epitope expressed by leukemia stem cells. Leukemia Research, 2014, 38, 1367-1373.	0.8	16
97	Depot system for controlled release of gold nanoparticles with precise intratumoral placement by permanent brachytherapy seed implantation (PSI) techniques. International Journal of Pharmaceutics, 2016, 515, 729-739.	5.2	16
98	Positron-Emission Tomography of HER2-Positive Breast Cancer Xenografts in Mice with ⁸⁹ Zr-Labeled Trastuzumab-DM1: A Comparison with ⁸⁹ Zr-Labeled Trastuzumab. Molecular Pharmaceutics, 2018, 15, 3383-3393.	4.6	16
99	Radioimmunotherapy of PANC-1 Human Pancreatic Cancer Xenografts in NRG Mice with Panitumumab Modified with Metal-Chelating Polymers Complexed to ¹⁷⁷ Lu. Molecular Pharmaceutics, 2019, 16, 768-778.	4.6	16
100	A comparison of DFO and DFO* conjugated to trastuzumab-DM1 for complexing 89Zr – In vitro stability and in vivo microPET/CT imaging studies in NOD/SCID mice with HER2-positive SK-OV-3 human ovarian cancer xenografts. Nuclear Medicine and Biology, 2020, 84-85, 11-19.	0.6	16
101	Monocyte chemotaxis mediated by formyl-methionyl-leucyl-phenylalanine conjugated with monoclonal antibodies against human ovarian carcinoma. International Journal of Immunopharmacology, 1983, 5, 307-314.	1.1	15
102	Comparisons of [18F]-1-deoxy-1-fluoro-scyllo-inositol with [18F]-FDG for PET imaging of inflammation, breast and brain cancer xenografts in athymic mice. Nuclear Medicine and Biology, 2011, 38, 953-959.	0.6	15
103	Biotinylated Polyacrylamide-Based Metal-Chelating Polymers and Their Influence on Antigen Recognition Following Conjugation to a Trastuzumab Fab Fragment. Biomacromolecules, 2012, 13, 2831-2842.	5.4	15
104	A radiolabeled antibody targeting CD123+ leukemia stem cells – initial radioimmunotherapy studies in NOD/SCID mice engrafted with primary human AML. Leukemia Research Reports, 2015, 4, 55-59.	0.4	15
105	Estrone-3-Sulphate, a Potential Novel Ligand for Targeting Breast Cancers. PLoS ONE, 2013, 8, e64069.	2.5	15
106	Antisense imaging of epidermal growth factor-induced p21 WAF-1/CIP-1 gene expression in MDA-MB-468 human breast cancer xenografts. European Journal of Nuclear Medicine and Molecular Imaging, 2003, 30, 1273-1280.	6.4	14
107	Preclinical pharmacokinetics, biodistribution, radiation dosimetry and acute toxicity studies required for regulatory approval of a Clinical Trial Application for a Phase I/II clinical trial of 1111n-BzDTPA-pertuzumab. Nuclear Medicine and Biology, 2015, 42, 78-84.	0.6	14
108	A comparison of non-biologically active truncated EGF (EGFt) and full-length hEGF for delivery of Auger electron-emitting 111 In to EGFR-positive breast cancer cells and tumor xenografts in athymic mice. Nuclear Medicine and Biology, 2015, 42, 931-938.	0.6	14

#	Article	IF	CITATIONS
109	Functionalization of Cellulose Nanocrystals with POEGMA Copolymers via Copper-Catalyzed Azide–Alkyne Cycloaddition for Potential Drug-Delivery Applications. Biomacromolecules, 2020, 21, 2014-2023.	5.4	14
110	Dual-Receptor-Targeted (DRT) Radiation Nanomedicine Labeled with ¹⁷⁷ Lu Is More Potent for Killing Human Breast Cancer Cells That Coexpress HER2 and EGFR Than Single-Receptor-Targeted (SRT) Radiation Nanomedicines. Molecular Pharmaceutics, 2020, 17, 1226-1236.	4.6	14
111	¹¹¹ In-Labeled Immunoconjugates (ICs) Bispecific for the Epidermal Growth Factor Receptor (EGFR) and Cyclin-Dependent Kinase Inhibitor, p27 ^{Kip1} . Cancer Biotherapy and Radiopharmaceuticals, 2009, 24, 163-173.	1.0	13
112	Kit for the preparation of 1111n-labeled pertuzumab injection for imaging response of HER2-positive breast cancer to trastuzumab (Herceptin). Applied Radiation and Isotopes, 2015, 95, 135-142.	1.5	13
113	Auger electron-emitting 111 In-DTPA-NLS-CSL360 radioimmunoconjugates are cytotoxic to human acute myeloid leukemia (AML) cells displaying the CD123 + /CD131 â^' phenotype of leukemia stem cells. Applied Radiation and Isotopes, 2016, 110, 1-7.	1.5	13
114	Advancing Novel Molecular Imaging Agents from Preclinical Studies to First-in-Humans Phase I Clinical Trials in Academia—A Roadmap for Overcoming Perceived Barriers. Bioconjugate Chemistry, 2015, 26, 625-632.	3.6	12
115	The Immunoreactivity of Radiolabeled Antibodies—Its Impact on Tumor Targeting and Strategies for Preservation. Cancer Biotherapy and Radiopharmaceuticals, 2004, 19, 669-672.	1.0	11
116	Integration of imaging into clinical practice to assess the delivery and performance of macromolecular and nanotechnology-based oncology therapies. Journal of Controlled Release, 2015, 219, 295-312.	9.9	11
117	Monte Carlo simulation of radiation transport and dose deposition from locally released gold nanoparticles labeled with ¹¹¹ In, ¹⁷⁷ Lu or ⁹⁰ Y incorporated into tissue implantable depots. Physics in Medicine and Biology, 2017, 62, 8581-8599.	3.0	11
118	Antiproliferative Effects of 1111n- or 177Lu-DOTATOC on Cells Exposed to Low Multiplicity-of-Infection Double-Deleted Vaccinia Virus Encoding Somatostatin Subtype-2 Receptor. Cancer Biotherapy and Radiopharmaceuticals, 2010, 25, 325-333.	1.0	10
119	Tumor uptake and tumor/blood ratios for [892r]Zr-DFO-trastuzumab-DM1 on microPET/CT images in NOD/SCID mice with human breast cancer xenografts are directly correlated with HER2 expression and response to trastuzumab-DM1. Nuclear Medicine and Biology, 2018, 67, 43-51.	0.6	10
120	MicroSPECT/CT Imaging of Cell-Line and Patient-Derived EGFR-Positive Tumor Xenografts in Mice with Panitumumab Fab Modified with Hexahistidine Peptides To Enable Labeling with ^{99m} Tc(I) Tricarbonyl Complex. Molecular Pharmaceutics, 2019, 16, 3559-3568.	4.6	10
121	Radioimmunotherapy of PANC-1 human pancreatic cancer xenografts in NOD/SCID or NRG mice with Panitumumab labeled with Auger electron emitting, 111In or β-particle emitting, 177Lu. EJNMMI Radiopharmacy and Chemistry, 2020, 5, 22.	3.9	10
122	Rapid imaging of human melanoma xenografts using an scFv fragment of the human monoclonal antibody H11 labelled with 1111n. Nuclear Medicine Communications, 2001, 22, 587-595.	1.1	9
123	Meta-[1231]iodobenzylguanidine is selectively radiotoxic to neuroblastoma cells at concentrations that spare cells of haematopoietic lineage. Nuclear Medicine Communications, 2004, 25, 1125-1130.	1.1	9
124	Construction and Evaluation of the Tumor Imaging Properties of123I-Labeled Recombinant and Enzymatically Generated Fab Fragments of the TAG-72 Monoclonal Antibody CC49. Bioconjugate Chemistry, 2007, 18, 677-684.	3.6	9
125	In vivo monitoring of intranuclear p27kip1 protein expression in breast cancer cells during trastuzumab (Herceptin) therapy. Nuclear Medicine and Biology, 2009, 36, 811-819.	0.6	9
126	Paradoxical effects of Auger electron-emitting 111 In-DTPA-NLS-CSL360 radioimmunoconjugates on hCD45 + cells in the bone marrow and spleen of leukemia-engrafted NOD/SCID or NRG mice. Nuclear Medicine and Biology, 2016, 43, 635-641.	0.6	8

#	Article	IF	CITATIONS
127	EGFR-Targeted Metal Chelating Polymers (MCPs) Harboring Multiple Pendant PEG2K Chains for MicroPET/CT Imaging of Patient-Derived Pancreatic Cancer Xenografts. ACS Biomaterials Science and Engineering, 2017, 3, 279-290.	5.2	7
128	Effectiveness and normal tissue toxicity of Auger electron (AE) radioimmunotherapy (RIT) with [111In]In-Bn-DTPA-nimotuzumab in mice with triple-negative or trastuzumab-resistant human breast cancer xenografts that overexpress EGFR. Nuclear Medicine and Biology, 2020, 80-81, 37-44.	0.6	7
129	Dose predictions for [177Lu]Lu-DOTA-panitumumab F(ab′)2 in NRG mice with HNSCC patient-derived tumour xenografts based on [64Cu]Cu-DOTA-panitumumab F(ab′)2 – implications for a PET theranostic strategy. EJNMMI Radiopharmacy and Chemistry, 2021, 6, 25.	3.9	5
130	The pharmaceutical stability of trastuzumab after short-term storage at room temperature assessed by analytical techniques and tumour imaging by microSPECT/CT. International Journal of Pharmaceutics, 2020, 588, 119786.	5.2	4
131	Cellular dosimetry of ¹⁹⁷ Hg, ^{197m} Hg and ¹¹¹ In: comparison of dose deposition and identification of the cell and nuclear membrane as important targets. International Journal of Radiation Biology, 2023, 99, 53-63.	1.8	4
132	Radioimmunotherapy of human pancreatic cancer xenografts in NOD-scid mice with [64Cu]Cu-NOTA-panitumumab F(ab′)2 alone or combined with radiosensitizing gemcitabine and the PARP inhibitor, rucaparib. Nuclear Medicine and Biology, 2020, 84-85, 46-54.	0.6	4
133	Compartmental analysis of the pharmacokinetics of radioiodinated monoclonal antibody B72.3 in colon cancer patients. Nuclear Medicine and Biology, 1993, 20, 57-64.	0.6	3
134	Fusion of the CH1 Domain of IgG1to Epidermal Growth Factor (EGF) Prolongs its Retention in the Blood but Does Not Increase Tumor Uptake. Cancer Biotherapy and Radiopharmaceuticals, 2002, 17, 665-671.	1.0	3
135	Aiming for a Direct Hit: Combining Molecular Imaging with Targeted Cancer Therapy. Journal of Nuclear Medicine, 2009, 50, 1017-1019.	5.0	3
136	The Radiopharmaceutical Science of Monoclonal Antibodies and Peptides for Imaging and Targetedin situ Radiotherapy of Malignancies. , 0, , 883-942.		2
137	Synthesis of a metal-chelating polymer with NOTA pendants as a carrier for 64Cu, intended for radioimmunotherapy. European Polymer Journal, 2020, 125, 109501.	5.4	2
138	Imaging of HER2-Positive Tumors in NOD/SCID Mice with Pertuzumab Fab-Hexahistidine Peptide Immunoconjugates Labeled with [99mTc]-(I)-Tricarbonyl Complex. Molecular Imaging and Biology, 2021, 23, 495-504.	2.6	2
139	Feasibility Evaluation of Radioimmunoguided Surgery of Breast Cancer. International Journal of Molecular Imaging, 2012, 2012, 1-10.	1.3	1
140	Immuno-PET to Optimize the Dose of Monoclonal Antibodies for Cancer Therapy: How Much Is Enough?. Journal of Nuclear Medicine, 2019, 60, 899-901.	5.0	1
141	Changing Surface Polyethylene Glycol Architecture Affects Elongated Nanoparticle Penetration into Multicellular Tumor Spheroids. Biomacromolecules, 2022, 23, 3296-3307.	5.4	1
142	A New Radioligand for the Epidermal Growth Factor Receptor:  111In Labeled Human Epidermal Growth Factor Derivatized with a Bifunctional Metal-Chelating Peptide. Bioconjugate Chemistry, 1996, 7, 721-721.	3.6	0
143	Site-Specific Conjugation of Metal-Chelating Polymers to Anti-Frizzled-2 Antibodies via Microbial Transglutaminase. Biomacromolecules, 2021, 22, 2491-2504.	5.4	0
144	Highlight selection of radiochemistry and radiopharmacy developments by editorial board. EJNMMI Radiopharmacy and Chemistry, 2021, 6, 31.	3.9	0

#	Article	IF	CITATIONS
145	MicroSPECT/CT Imaging of Human Leukemia Engraftment In NOD-Scid Mice Using [111In]-Labeled 7G3 Anti-CD123 Antibodies. Blood, 2010, 116, 968-968.	1.4	0
146	Irradiated NK-92 Targets AML Leukemic Stem Cells in Vivo and Gene-Modified CD16+NK-92 Mediates Antibody Dependent Cell Mediated Cytotoxicity (ADCC) Against CD123+ Cells. Blood, 2012, 120, 1909-1909.	1.4	0